We are IntechOpen,
the world's leading publisher of
Open Access books
Built by scientists, for scientists

4,800
Open access books available

122,000
International authors and editors

135M
Downloads

Our authors are among the

154
Countries delivered to

TOP 1%
most cited scientists

12.2%
Contributors from top 500 universities

CLARIVATE ANALYTICS
BOOK CITATION INDEX
INDEXED

WEB OF SCIENCE™

Selection of our books indexed in the Book Citation Index
in Web of Science™ Core Collection (BKCI)

Interested in publishing with us?
Contact book.department@intechopen.com

Numbers displayed above are based on latest data collected.
For more information visit www.intechopen.com

Indoor Air Control by Microplasma

Kazuo Shimizu
Shizuoka University
Japan

1. Introduction

Sick-Building Syndrome (SBS) has become an environmental issue worldwide in recent decades (P. Burge, 2004). Much research on this syndrome has been carried out. Generally, it is known that since buildings became more airtight for improvement of air-conditioning and heating, the effect of Volatile Organic Compounds (VOCs) diffusions from building materials has increased, causing many symptoms of SBS. Control of these indoor air pollutants is necessary to maintain Indoor Air Quality (IAQ). Recently, Indoor Air Quality (IAQ) is recognized as an important factor of home and building construction (P. Wolkoff, G. D.Nielsen, 2001).

Formaldehyde (HCHO) is one of the most common indoor VOCs. This substance is emitted from resins, plastics and often building materials, such as plywood, chipboard, and paneling, and is one of the main causes of SBS (H. Yoshino, 2004). Indoor air contaminants which worsen IAQ are characterized by the presence of not only VOCs, but also of fungus and bacteria, various malodorous substances and Environmental Tobacco Smoke (ETS) etc. VOCs such as formaldehyde (HCHO) are well known as a cause of sick building syndrome (A. Seki et al., 2007). Indoor air concentration of HCHO is regulated at 0.08 ppm by Ministry of Health, Labor and Welfare (MHLW) in Japan. Decompositions of VOCs by nonthermal plasma technique have been researched recently (A. Koutsospyros et al., 2004; D. Li et al., 2002; K. N. Faungnawakji et al., 2004; K. Urashima and J. S. Chang, 2000; T. Oda et al., 2004; Y.-H. Song et al., 2002).

In addition, infective diseases such as new influenza strains caused by pathogenic organisms have been spread worldwide. Recently this causes serious problems in schools and a lack of vaccines in many countries. In this context, home appliance manufactures have developed air purifiers for the market in Japan, but not in the market worldwide (Sharp, Panasonic, Daikin). Research on air purification; both odor treatment and bacteria, viruses treatment based on the nonthermal plasma technique has also been intensively studied in universities as well as by home appliance manufacturers (A. Sakudo and H. Shintani, 2010; F. J. Trompeter et al., 2002; H. Ghomi et al., 2005; K. Kitano et al., 2006; M. Laroussi et al., 2004; M. Nagatsu et al., 2003; T. C. Montie et al., 2000, N. Hayashi et al., 2006; N. S. Panikov et al., 2002, T. Ito et al., 1992.)

These nonthermal plasma techniques were carried out with rather "high voltage" region (5-15 kV, sometimes more than 20 kV)(A. Mizuno et al., 1995). It is expected that they can be alternatives to other simple plasma techniques to purify indoor air. In this chapter, a technique for indoor air control by microplasma will be introduced (K. Shimizu et al., 2008, 2009, and 2010 a, b, and c).

2. About microplasma

Atmospheric microplasma is a type of dielectric barrier discharge (DBD) (K. Tachibana, 2006; L. A. Rosocha et al., 1993; S. Agnihotri et al., 2004; U. Kogelschatz, 2007). The discharge gap is set to an order of micrometers which is extremely narrow, enabling the plasma to generate at a discharge voltage of around 600 V. Streamers between the electrodes are also very small (in the order of micrometers), resulting in a relatively compact and dense plasma. Fig. 1 is an image of the microplasma during discharge. Streamers were generated not only between the electrodes but also around the holes of the electrodes.
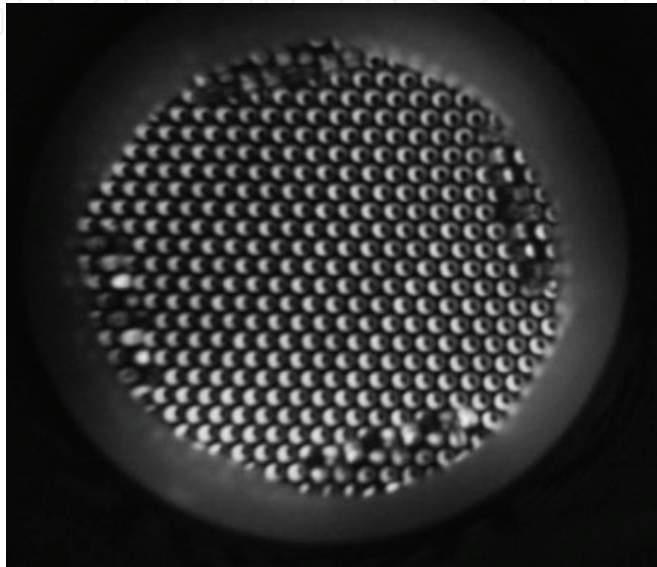

Fig. 1. Image of the microplasma electrode (Vd=1 kV, front view). A photo taken by a digital camera with 5 seconds of shutter opening.

Discharge gap was set based on Paschen's law, which indicates the minimum sparking voltage and discharge gap for various gases at atmospheric pressure. High reduced electric fields were readily obtainable with such small discharge gaps, resulting in a reduction of low energy electrons (1-2 eV), which dissociate ozone (B. Eliasson et al., 1987; J. Kitayama and M. Kuzumoto, 1997). This microplasma electrode has the advantage of generating a high concentration of ozone with low discharge voltage and power.

Fig. 2 shows the schematic image of microplasma electrodes for odor treatment (K. Shimizu et al., 2010b).

3. Experimental setup

3.1 Microplasma electrode and reactors

Fig. 2 is a schematic image of the microplasma electrode. Two perforated metal plates covered with dielectric materials were faced together, and an alternating voltage (about 25 kHz, 1 kV) was applied. Pulse power supply can also be used, a technique detailed in 3.2, 3.3, and 3.4. Innumerable streamers generated between the electrodes, which could excite various radicals (O*, N*, etc) and generate ozone. These radicals could react with the flowed gas and detoxify it (H. X. Din et al., 2005). The electrode had a diameter of 45 to 60 mm and a thickness of 1 mm. Since this electrode had a large aperture (aperture ratio: about 30 to 40%),

the pressure loss through the electrode was extremely low (less than 5 mmH$_2$O at gas flow rate 10 L/min). This could enable large volume gas treatment passes.
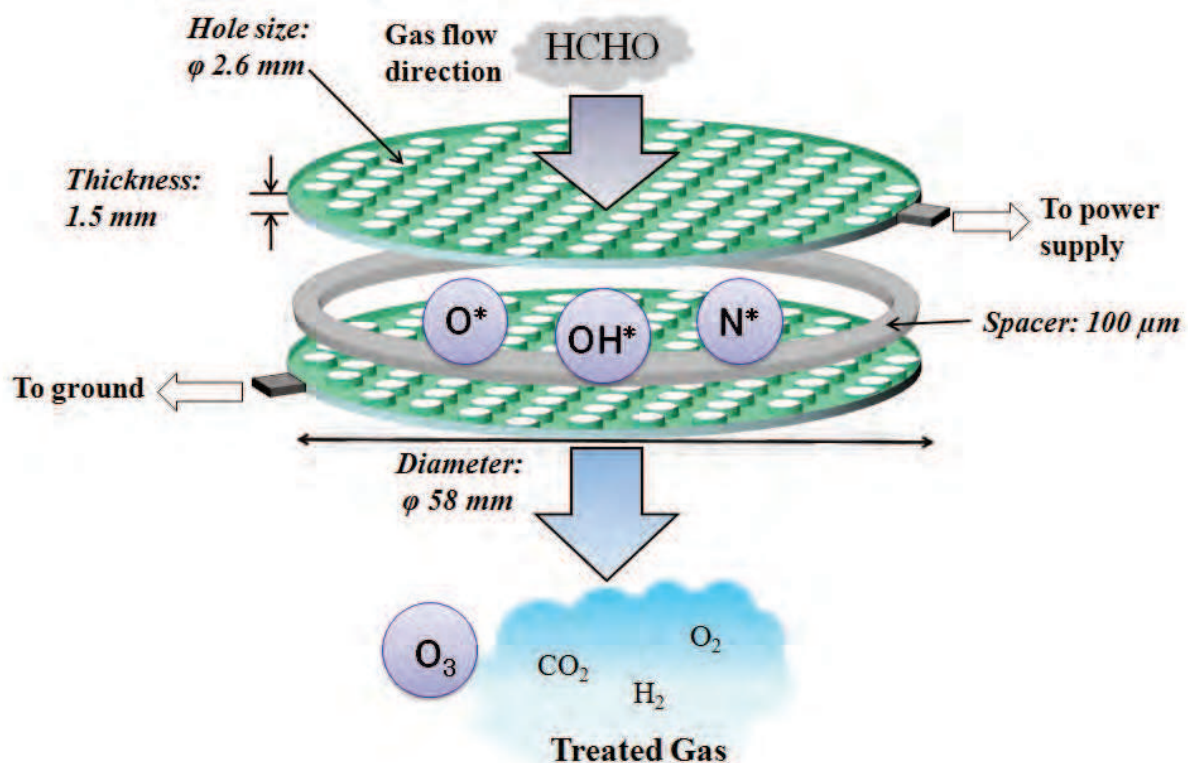

Fig. 2. Schematic image of microplasma electrodes for treating odor molecules. The pressure loss between the electrodes is very small.
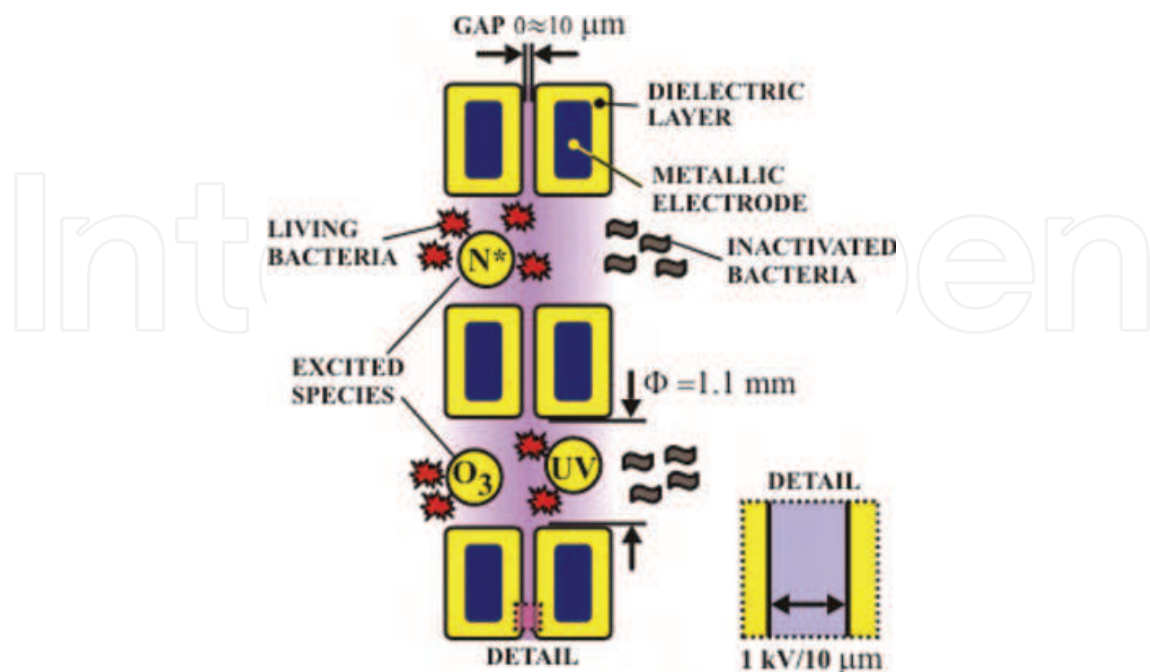

Fig. 3. Schematic image of the sterilization process of microplasma between the electrodes.

Fig. 3 shows a schematic image of the active species generated by the microplasma between the electrodes and the exposure of the living bacteria to the microplasma causing sterilization. A suspension of living bacteria in water was sprayed perpendicular to the electrode. The living bacteria were carried through the holes by the carrier gas. Due to the small discharge gap between electrodes (0–10 μm) and the direction of the gas flow, few of the bacteria enter the discharge gap between electrodes, and most pass through the holes. The few bacteria that enter the narrow zone between the electrodes attach to the surface of the electrodes and are lost from the flow of the carrier gas. The bacteria and their colonies that were counted on the nutrient medium were exclusively those bacteria which passed through the holes.
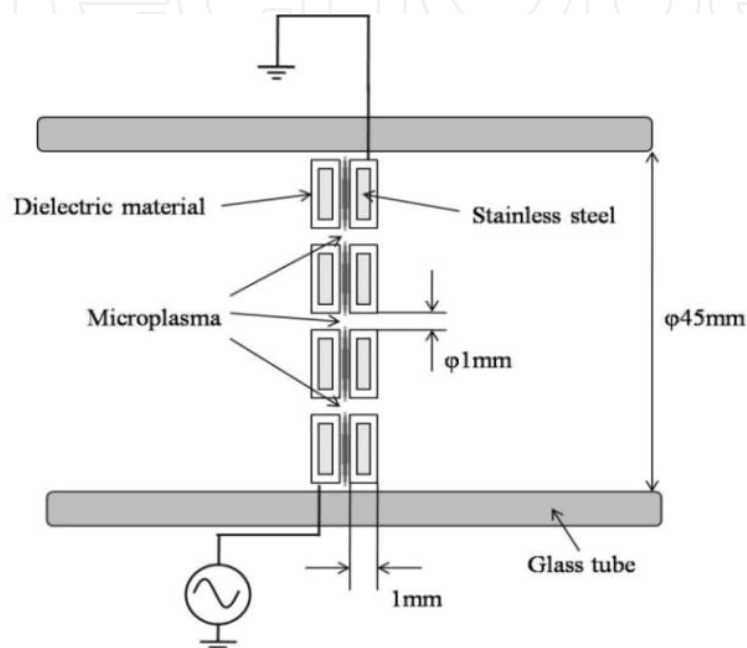

Fig. 4. Schematic image of the microplasma reactor (side view).The discharge gap is about 10 to 100 μm with or without a spacer.
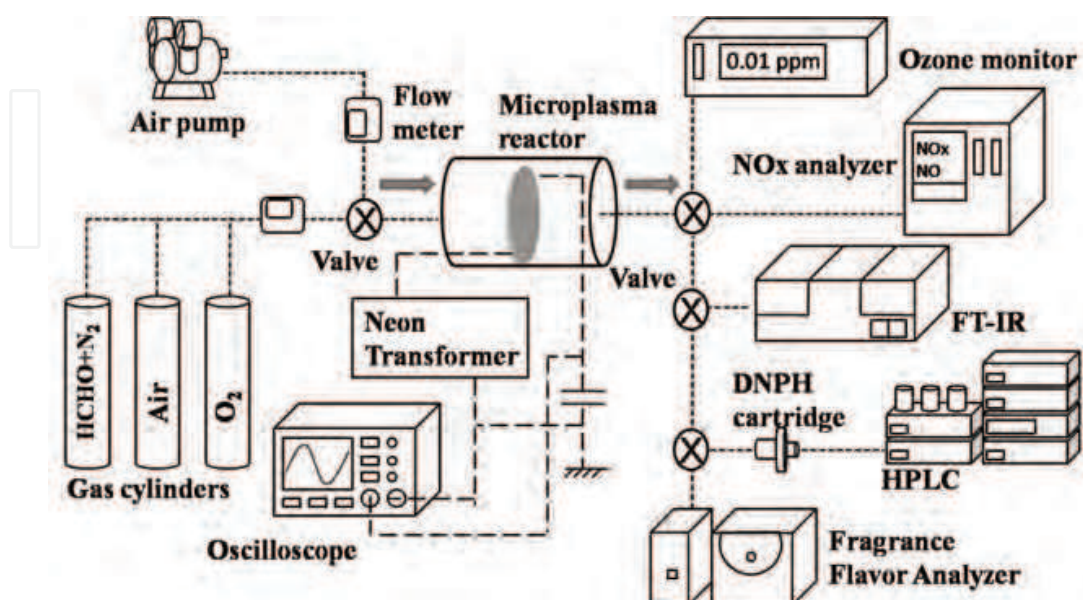

Fig. 5. An experimental setup for one pass process of formaldehyde removal.

Fig. 4 shows the microplasma reactor, and the experimental setup for VOCs removal is presented in Fig. 5. In this experiment, formaldehyde was used as VOCs. Air was flowed into diluted formalin solution by an air pump or gas cylinders, supplying a constant low concentration of formaldehyde to the microplasma reactor.

The treated gas was then sent to an ozone monitor (Ebara Jitsugyo, EG-2001B), NOx analyzer (Shimadzu, NOA-7000), FTIR (Shimadzu, IRPrestige-21), HPLC (Agilent, 1100 series) and Fragrance Flavor Analyzer (Shimadzu, FF-2A) for investigation of the gas composition change, identification and quantity analysis of by-products, and distinction of the gas smell.

Also, an oscilloscope (Tektronix, TDS 3014) was used to measure the discharge voltage, current, and power. Lissajous figures were used for the estimation of discharge power.
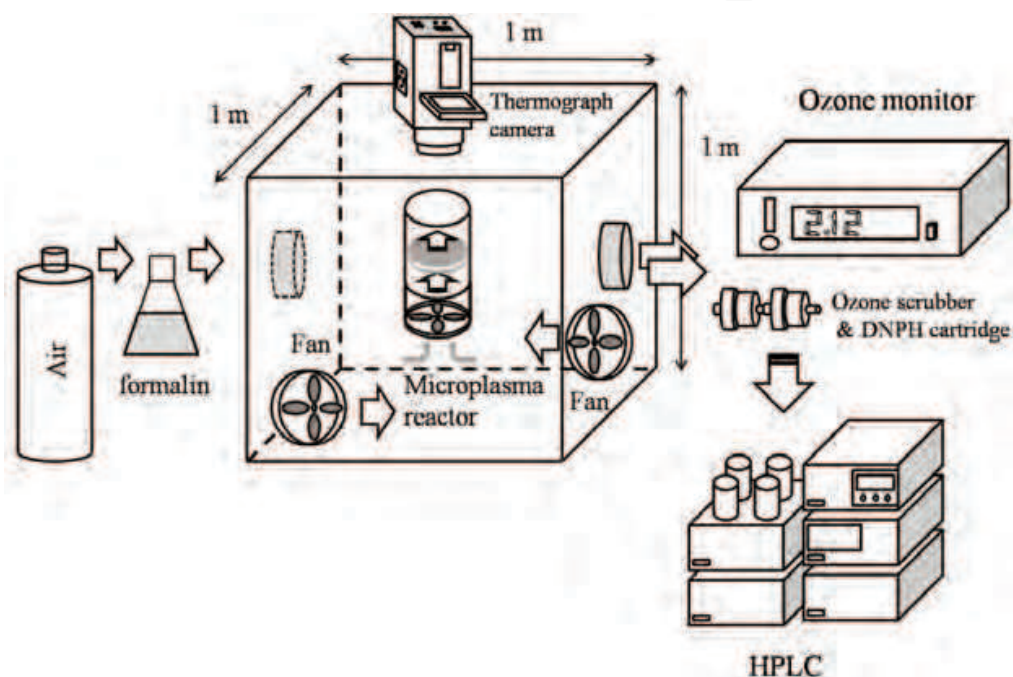

Fig. 6. An experimental setup for large volume process of VOCs removal.

The experimental setup for large volume treatment of VOCs is shown in Fig. 6. Formalin solution (abt. HCHO 37 %) was used to generate 0.5 ppm in 1 m^3 acrylic chamber. The inside gas was treated by microplasma reactor at a gas flow rate of 1,500 L/min. Before the microplasma treatment a fan was used to equalize the concentration of HCHO in the whole volume. Treatment time was 60 minutes; HCHO and O_3 concentration was measured each 12 minutes by ozone monitor and HPLC. The discharge voltage of an HV amplifier and Marx Generator circuit was set at 1.2 kV, and frequency of both power sources was set at 1.5 kHz. These power supplies are explained in the next section.

Sterilization effect of bacteria at low voltage by using atmospheric microplasma was also investigated. *Escherichia coli* JCM20135 and *Bacillus subtilis* JCB20036 were used as the target to be sterilized. An experimental setup for sterilization of bacteria is shown in Fig. 7.

This Bacteria sterilization described here by microplasma was a one pass process. The liquid culture medium was introduced in the microplasma reactor and sprayed at a gas flow rate of 3.5 L/min by use of a medical nebulizer, through the electrode against a petri dish with culture medium. Carrier gas was also introduced in the reactor at a gas flow rate

of 5 L/min. After the experiment, the laboratory dishes were incubated in the incubator at 37°C for 15 hours after microplasma treatment. Sterilization effect of microplasma was inspected by comparing the number of colonies with and without microplasma treatment.
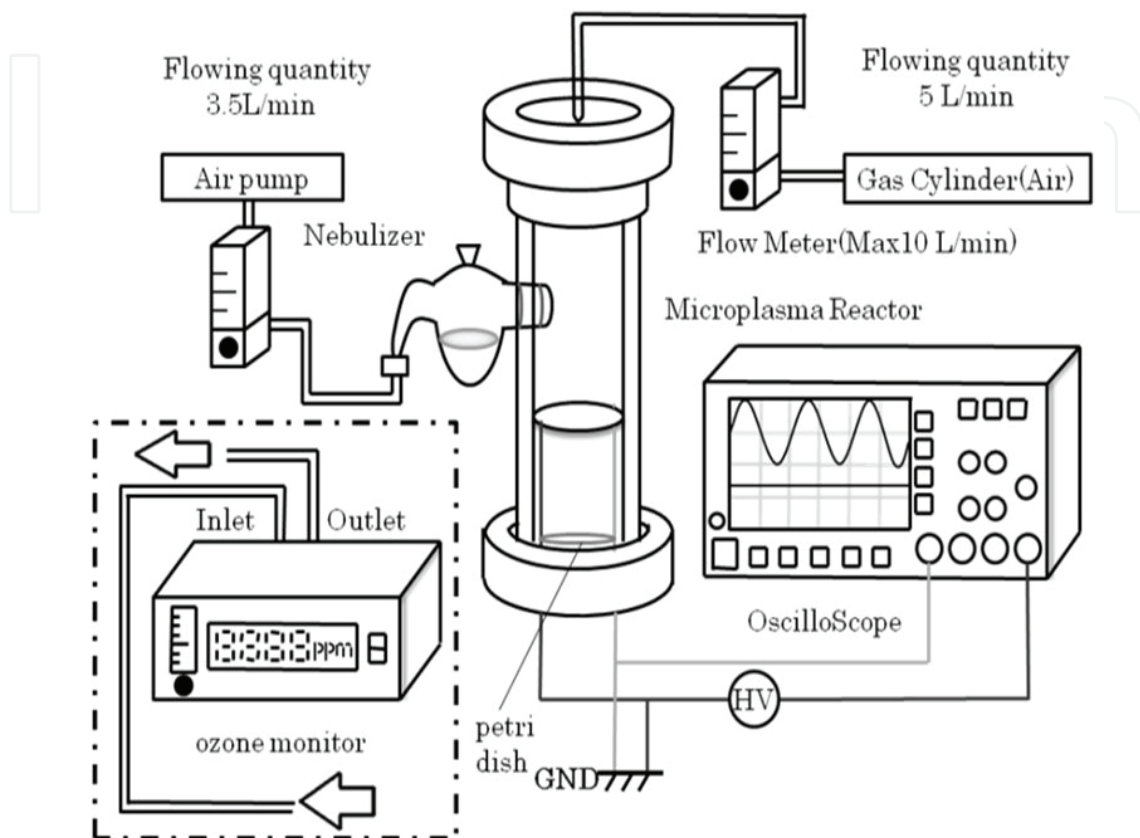

Fig. 7. An experimental setup for bacteria sterilizaion.

3.2 Power supply

In another series of experiments, high frequency AC neon transformer (LECIP, M-1H shown in Fig. 8), a pulse power supply consisting of a function generator (Tektronix, AFG3021B) and high voltage amplifier (Trek, MODEL 5/80) were also used as power supplies to energize the electrodes.

A Marx Generator with MOSFET switches was developed as a pulse power supply. It generates negative pulses up to – 1.6 kV, rise time 100 ns and pulse width 1.5 μs. The electronic circuit of Marx Generator with 2 stages is shown in Fig. 9.

When the MOSFET switches are opened, the capacitors are linked in parallel connection and charged at a value V. By turning on the MOSFET switches, the capacitors discharge in a series connection. Thus the output voltage has the value V multiplied with the number of capacitors, in this case 2V (M. Blajan et al., 2010). The DC power source which charges the capacitors has a maximum output of 0.8 kV, thus the Marx Generator can generate negative pulses up to -1.6 kV.

It is worth mentioning that the power supply was small and easy to handle, generating microplasma as shown in Figs. 8 and 10.
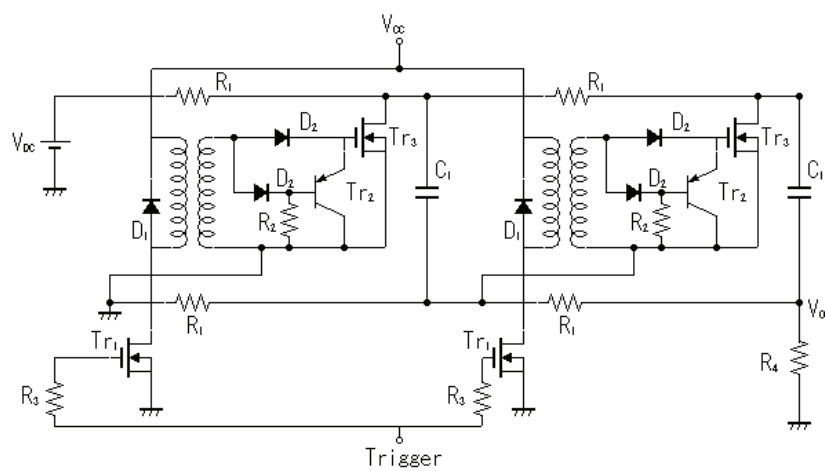
Fig. 8. A small AC power supply.

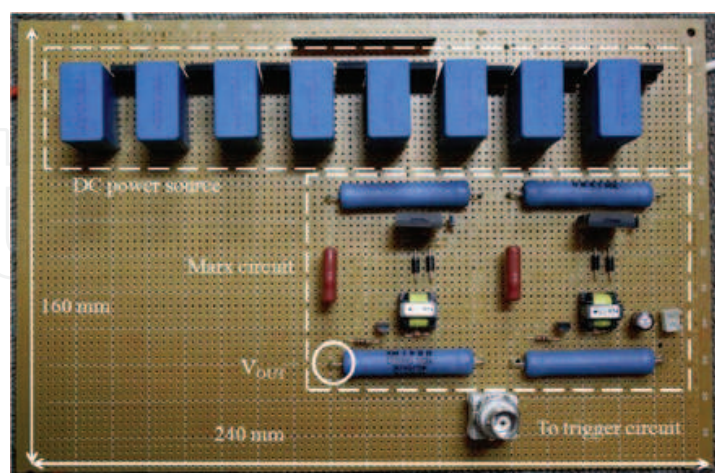Fig. 9. Example of a negative pulse Marx Generator circuit.

Fig. 10. Image of a Marx Generator circuit.

3.3 Waveforms for generating microplasma

Figure 11 shows the typical waveform of discharge voltage and corresponding discharge current generating microplasma at about 1 kV. This waveform shows alternate current and

frequency is about 25 kHz. Corresponding discharge current showed a typical waveform of dielectric barrier discharge. The microplasma reactor can generate atmospheric plasma at about 1 kV, since its discharge gap was narrow (about 50 μm) (K. Shimizu et al., 2008, 2009, and 2010a and b).
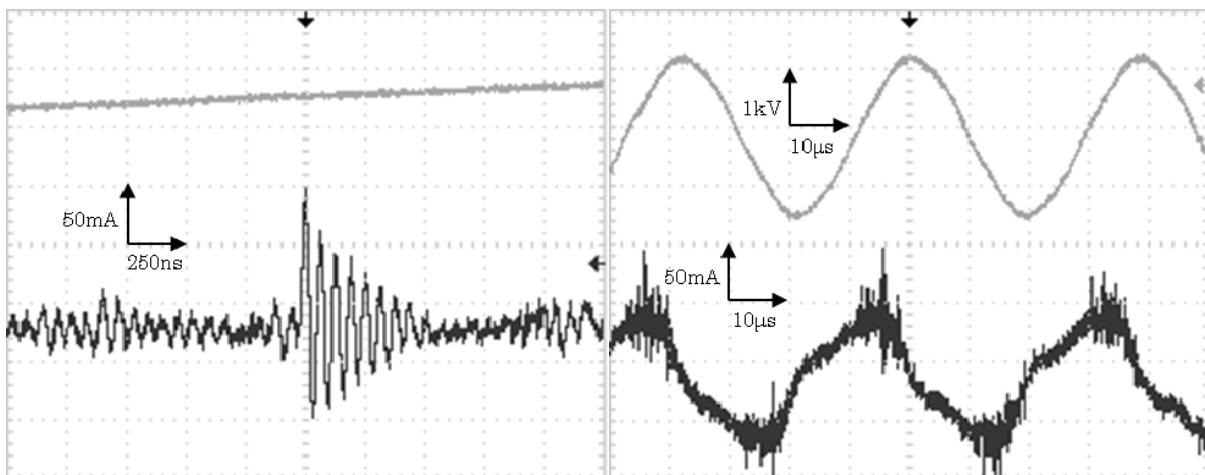

Fig. 11. Typical waveform of microplasma with AC neon transformer; applied voltage (above) and corresponding discharge current (below). Time scale; 10 μs (left), 250 ns (right).
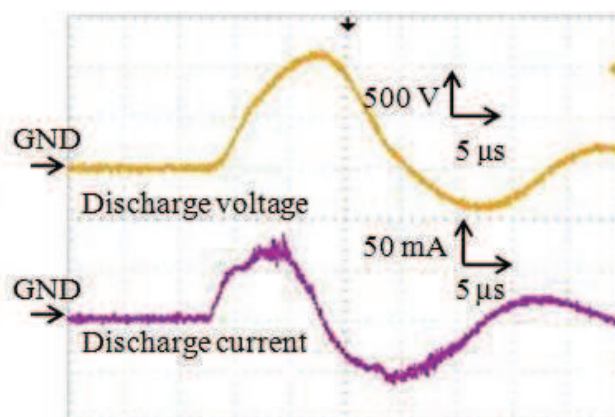

Fig. 12. Discharge voltage and corresponding discharge current by a high voltage amplifier.

Pulse voltage was also applied to generate microplasma as shown in Figs. 12 and 13. Repetition frequency of both pulses was fixed to 1 kHz. The waveforms of pulse voltage generated by an HV amplifier are shown in Fig. 12. Spike currents occurred due to the streamers, convoluted on the current waveform, and were observed in addition to the capacitive current at the steepest slopes of the waveform.

The waveforms of pulse voltage by a Marx Generator circuit are shown in Fig. 13. Rise time of discharge voltage by a Marx Generator circuit was 100 ns, and fall time was 4 μs. Sharp discharge current was observed.

Waveforms are different from Figs. 11 to 13, and the microplasma generation was confirmed with all the applied voltage, since the microplasma was generated by typical dielectric barrier discharge. The indoor air control devices in the market are usually driven by weak corona discharge ranged from 5 to 10 kV without dielectric barriers on their electrodes. This is a significant difference between the microplasma technique under discussion here, and

the technique employed by indoor air control devices on the market now which generate ions, according to the manufacturers claims.
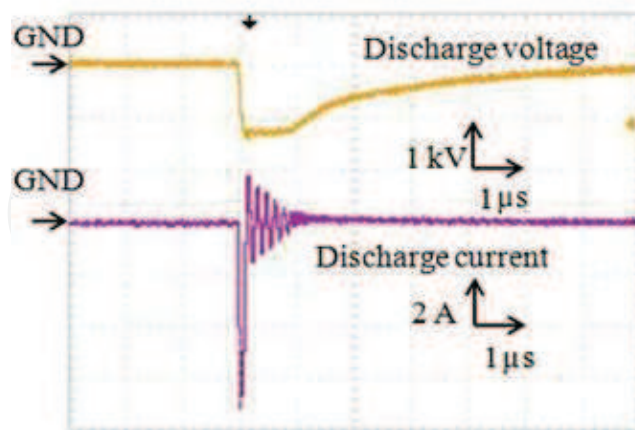

Fig. 13. Discharge voltage and corresponding discharge current by a Marx Generator.

3.4 Power consumption

The characteristic of discharge power versus discharge voltage is shown in Fig. 14. Discharge power was estimated by integrating the waveform of voltage and current product in time using an oscilloscope and dividing it with time in order to obtain the power for one cycle.
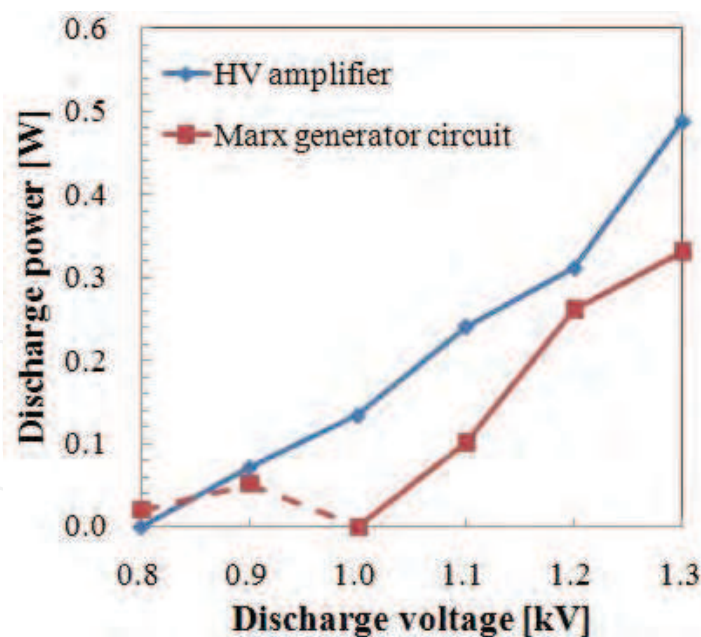

Fig. 14. Characteristic of discharge power by both power sources.

Discharge power of Marx Generator at 1.0 kV was lower than that at 0.9 kV. This could be explained by the decrease of transient form of the discharge current when microplasma discharge started to occur at 1 kV.

As the discharge voltage increases, the discharge power increases. Discharge power of an HV amplifier was 0.49 W at 1.3 kV for one cycle, and discharge power of Marx Generator

was 0.33 W. Discharge power could attributed to the ozone generation which will discuss in the next part.

4. Results and discussion

In this part, experimental results for indoor air control by microplasma is presented. First, control of VOCs in simulated indoor air will be introduced with a small quantity of ozone generation. After that byproduct analysis, chemical reactions will be discussed. Finally, bacteria in simulated indoor air will be presented. Mechanisms of sterilization process are also discussed along with data such as UV light emission by microplasma.

4.1 Removal of HCHO and ozone generation in air

The experimental results of HCHO removal in one pass process using a microplasma reactor (shown in Fig. 5)powered by a HV amplifier are shown in Fig. 15. Discharge voltage was set at 0.8 ~ 1.3 kV. The microplasma discharge started at 0.9 kV. Thus no HCHO removal was measured at 0.8 kV (initial concentration of HCHO: 0.707 ppm). The removal ratio of HCHO at 0.9 kV was 35.4 %. At this discharge voltage, ozone generation was initiated (about 0.2 ppm). As discharge voltage increased, the HCHO removal ratio and generated ozone concentration also increases. The HCHO removal ratio reached 95.8 % at the discharge voltage of 1.1 kV, and 3.46 ppm of ozone was generated at this voltage. The removal ratio of HCHO was saturated at around 96 % when the voltage was increased above 1.1 kV. Generated ozone concentration increased with discharge voltage. Thus the maximum value of ozone concentration was 12.1 ppm at 1.3 kV.
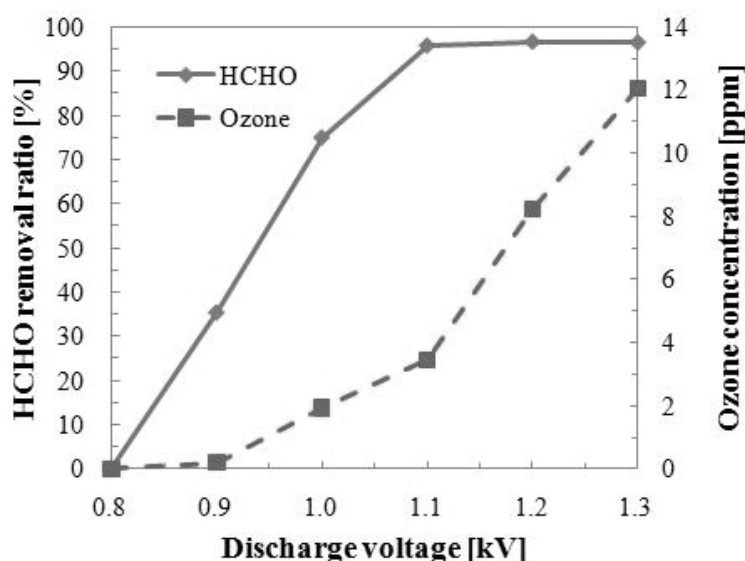

Fig. 15. HCHO and O_3 concentration in one pass process by an HV amplifier.

The optimal value for the discharge voltage, in the HCHO removal process when an HV amplifier was used, could be considered to be 0.9 kV due to the relatively high removal ratio and low generated ozone concentration.

The experimental results of HCHO removal in one pass process using a Marx Generator are shown in Fig. 16. Initial concentration of HCHO was set at 0.762 ppm. The removal ratio of

HCHO was 30.7% at 1.1 kV. At this discharge voltage, generation of ozone was confirmed (0.16 ppm), and was lower than with an HV amplifier. The HCHO removal ratio reached 96.2 % when discharge voltage increased to 1.3 kV. Generated ozone concentration of 3.81 ppm could be considered low compared to an HV amplifier results.
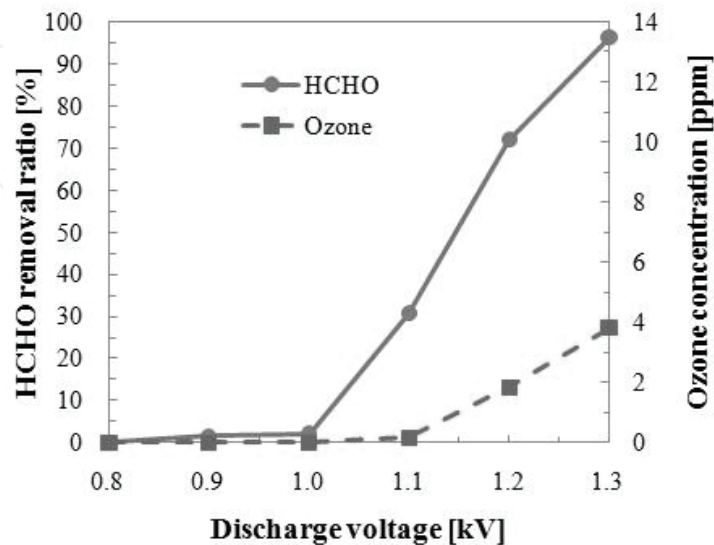

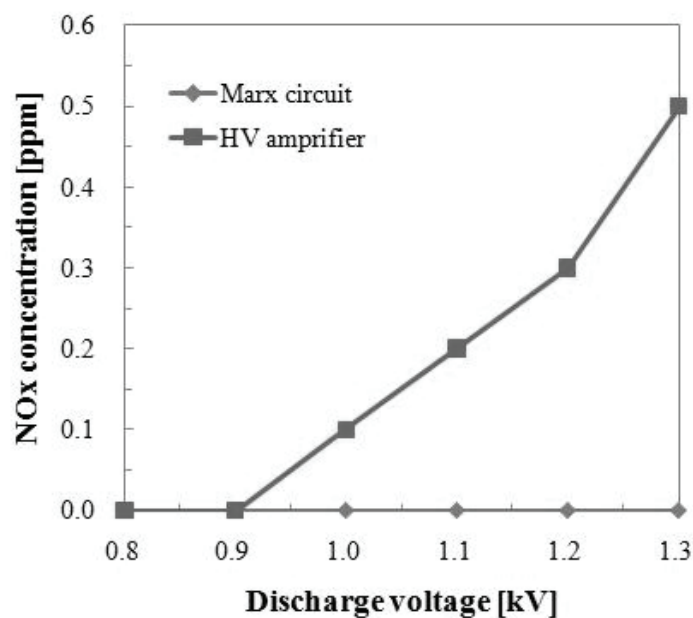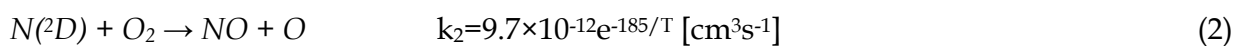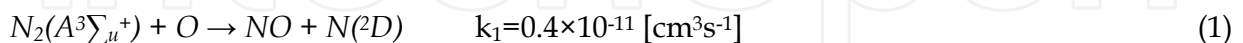Fig. 16. HCHO and O_3 concentration in one pass treatment by Marx Generator circuit.

Fig. 17. NOx generation difference by the pulse power supplies.

In the one pass HCHO removal process by microplasma, mixing HCHO from a gas cylinder with air from another gas cylinder was used as simulated indoor air. Thus the humidity of the mixed gas was 0%. Reaction process by microplasma with humidity will be presented bellow (Figs.19 and 20). This process could have OH radicals which play a role in leading oxidization reactions.

NOx generation characteristics by both power sources is shown in Fig. 17. When an HV amplifier was used, NOx started to be generated at 1.0 kV. After increasing the discharge voltage, the NOx concentration increased to 0.5 ppm at 1.3 kV. On the contrary, NOx generation was not observed when using a Marx Generator as the pulse power supply.

Atmospheric microplasma leads to the dissociation of nitrogen molecules to generate nitrogen atoms or meta stable state $N_2(A)$ molecules to produce NO as shown in equations (1) and (2) (A. Rousseau et al., 2005). Since NO production depends on the pulse duty cycle ratio, which is proportional to the pulse power, microplasma powered by short pulses could not be responsible for the NOx generation because of low pulse duty cycle ratio, even at the voltage as high as 1.3 kV.

$$N_2(A^3\textstyle\sum_u{}^+) + O \rightarrow NO + N(^2D) \qquad k_1=0.4\times10^{-11} \text{ [cm}^3\text{s}^{-1}] \tag{1}$$

$$N(^2D) + O_2 \rightarrow NO + O \qquad k_2=9.7\times10^{-12}e^{-185/T} \text{ [cm}^3\text{s}^{-1}] \tag{2}$$

Considering that NOx are well known for their toxicity, in a further implementation of microplasma as a technology for cleaning the room air, a Marx Generator could be favorable to use as the solution for the power supply.
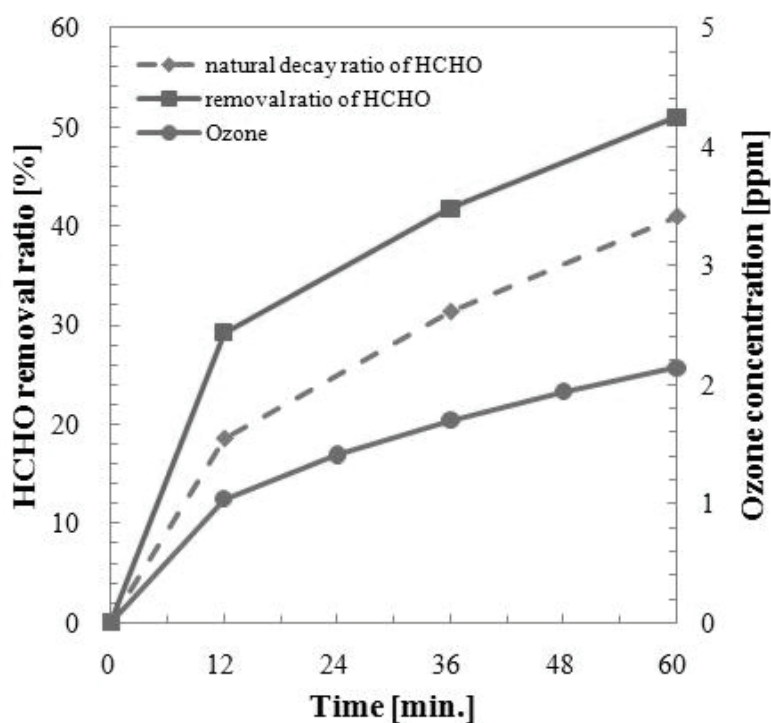

Fig. 18. Large volume HCHO treatment by an HV amplifier.

The results of large volume HCHO treatment using 1 m³ chamber (shown in Fig. 6, gas flow rate: 1,500 L/min.) with an HV amplifier as a power supply are shown in Fig. 18. In this case, the sample HCHO gas was generated from the evaporation of formalin in room air. The gas humidity was equivalent to room air (abt. 60 %).

The removal ratio and generated ozone concentration increased with the treatment time. A natural decay of HCHO concentration was measured (Fig. 18). The natural decay after 60 minutes was 41 % and the removal ratio of HCHO with microplasma reached 51 %. Initial concentration of HCHO was set at 0.537 ppm and after 60 minutes of microplasma treatment 0.05 ppm of HCHO was removed, also taking into consideration the effect of

natural decay. The generated ozone concentration was 2.14 ppm in the chamber after 60 minutes of microplasma treatment.
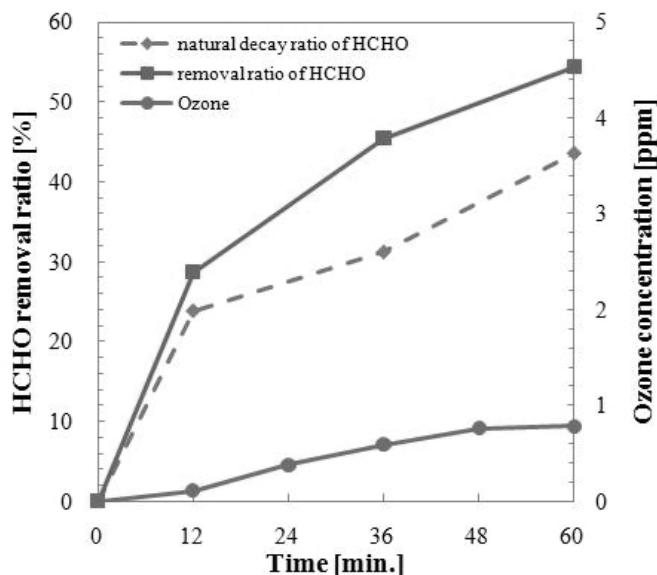

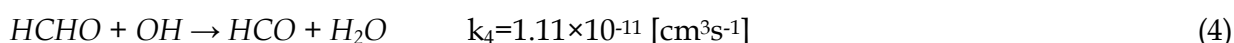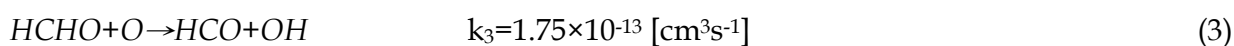Fig. 19. Large volume HCHO treatment by Marx Generator.

The results of large volume HCHO treatment using a Marx Generator to energize the microplasma electrodes are shown in Fig. 19. The natural decay ratio was 43.6 %, and the removal ratio of HCHO reached 54.4 % after 60 minutes of treatment. Generated ozone concentration was 0.78 ppm after the same period of time. HCHO removal ratio was comparable with the removal ratio obtained with an HV amplifier as a power supply; however, the generated ozone concentration was lower.

The results obtained with a Marx Generator are similar in both treatment cases (with one pass reactor and large reactor) from the point of view of HCHO removal ratio, but the NOx and ozone generation are lower. Thus it can be concluded that the use of a Marx Generator as a power supply has advantages over than that of an HV amplifier.

HCHO concentration of actual houses is usually below 0.1 ppm. Removal performance of HCHO by microplasma treatment at large gas flow rate was about 0.05 ppm. This recommends microplasma technology as a solution for the treatment of indoor air contaminants.

4.2 Byproduct analysis and reaction process by microplasma

There are many reports on treating hazardous substances, such as cigarette smoke and VOCs (H. Yoshida et al., 1989, T. Kuroki et al., 2001, R.Atkinson et al., 2004, 2006). Most of these methods require high voltages and have difficulty handling large volume. Therefore, we have carried out HCHO removal in simlated indoor air experimentally using a microplasma reactor, which is more compact, and has low energy consumption. Major plasma chemical reactions are known in the treatment of HCHO are as follows (D. G. Storch and M. J. Krushner, 1993):

$$HCHO+O \rightarrow HCO+OH \qquad k_3=1.75\times10^{-13} \text{ [cm}^3\text{s}^{-1}\text{]} \qquad (3)$$

$$HCHO + OH \rightarrow HCO + H_2O \qquad k_4=1.11\times10^{-11} \text{ [cm}^3\text{s}^{-1}\text{]} \qquad (4)$$

$$HCO + O \rightarrow CO_2 + H \qquad k_5=5.00\times10^{-11} \text{ [cm}^3\text{s}^{-1}] \qquad (5)$$

$$HCO + O \rightarrow CO + OH \qquad k_6=5.00\times10^{-11} \text{ [cm}^3\text{s}^{-1}] \qquad (6)$$

$$HCO + OH \rightarrow H_2O + CO \qquad k_7=5.00\times10^{-11} \text{ [cm}^3\text{s}^{-1}] \qquad (7)$$
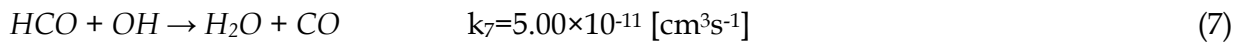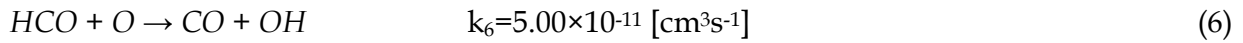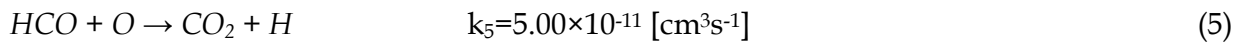
Fig. 20 and 21 are the analysis results obtained by the FTIR. In this case, the initial concentration of HCHO was set to 10 ppm to observe the spectrum difference clearly, and the discharge voltage was set to 600, 800, and 1000 V with an AC neon transformer. The gas flow rate was set to 2.0 L/min and humidity conditions were changed.
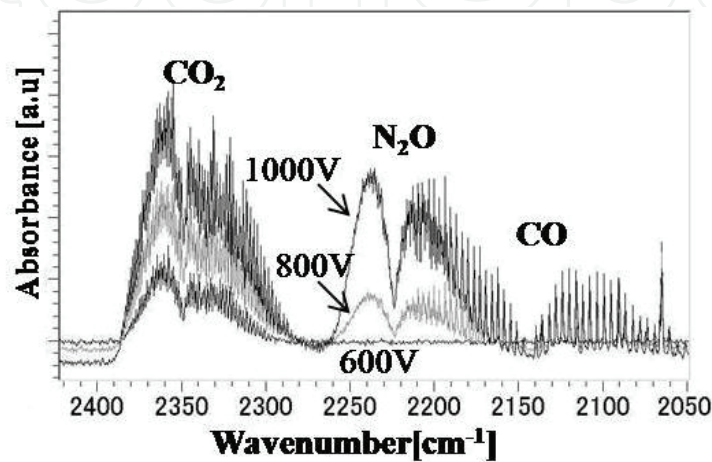

Fig. 20. FT-IR analysis (2000-2450 cm^{-1}) after formaldehyde treatment without humidity (0%) in the flowing air.
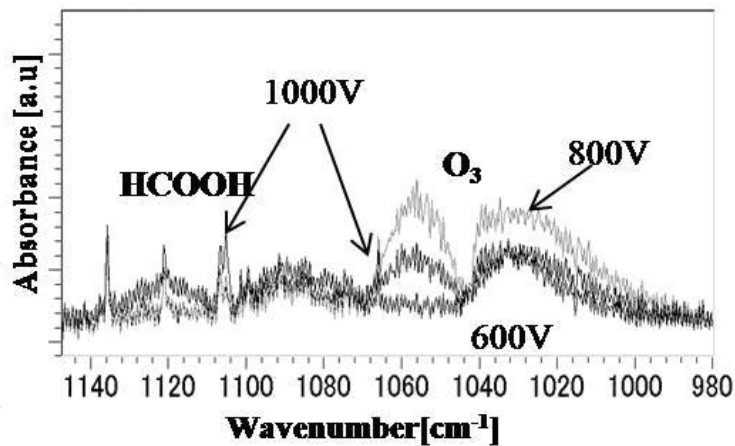

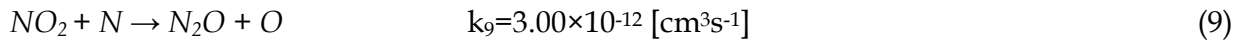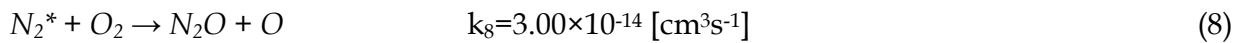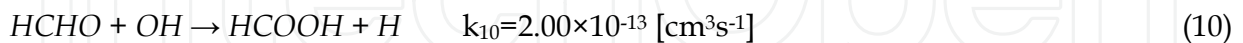Fig. 21. FT-IR analysis afterformaldehyde treatment with humidity (60%) in the flowing air.

From the analysis results, carbon dioxide (CO$_2$: 2250-2400 [cm^{-1}]), carbon monoxide (CO: 2000-2250 [cm^{-1}]) and nitrous oxide (N$_2$O: 2175-2250 [cm^{-1}]) were discovered as byproducts in zero humidity air conditions. CO$_2$ and CO could be a result of equations (5-7). The generation of N$_2$O according to (8) is realized by the reaction of excited species of N$_2$ with O$_2$. The presence of N$_2$ excited species in microplasma was demonstrated by the measurement of N$_2$ second positive band system and N$_2$$^+$ first negative band system for microplasma discharge in air (M. Blajan et al., 2009). N$_2$O was a byproduct which derives also from reaction (9).

$$N_2^* + O_2 \rightarrow N_2O + O \qquad\qquad k_8 = 3.00 \times 10^{-14} \ [cm^3 s^{-1}] \tag{8}$$

$$NO_2 + N \rightarrow N_2O + O \qquad\qquad k_9 = 3.00 \times 10^{-12} \ [cm^3 s^{-1}] \tag{9}$$

When there was humidity in the flowing air, formic acid (HCOOH: 1100 $[cm^{-1}]$) is also confirmed as a byproduct (Fig.19). Electron impact dissociation of H_2O leads to the production of H and OH radicals and also to excited state $O(^1D)$ dissociated H_2O to generate OH a process described bellow (4.5). Thus formaldehyde reacts with generated OH radicals, and HCOOH was formed from the following equation:

$$HCHO + OH \rightarrow HCOOH + H \qquad k_{10} = 2.00 \times 10^{-13} \ [cm^3 s^{-1}] \tag{10}$$

It is not desirable to produce byproducts which are harmful to humans. Therefore, there should either be a second treatment process for these byproducts, or the electron energy should be controlled in order not to dissociate N_2 and CO_2. These issues will be investigated and could be controlled by a power supply.

4.3 Smell analysis

HCHO is known to have a sweet smell, and can be detected when there is 0.08 ppm or more in the air. After microplasma treatment, a few byproducts were confirmed. This fact suggests the smell of the treated gas could also be changed. A smell analysis was carried out to confirm the difference of smell before and after the microplasma treatment.
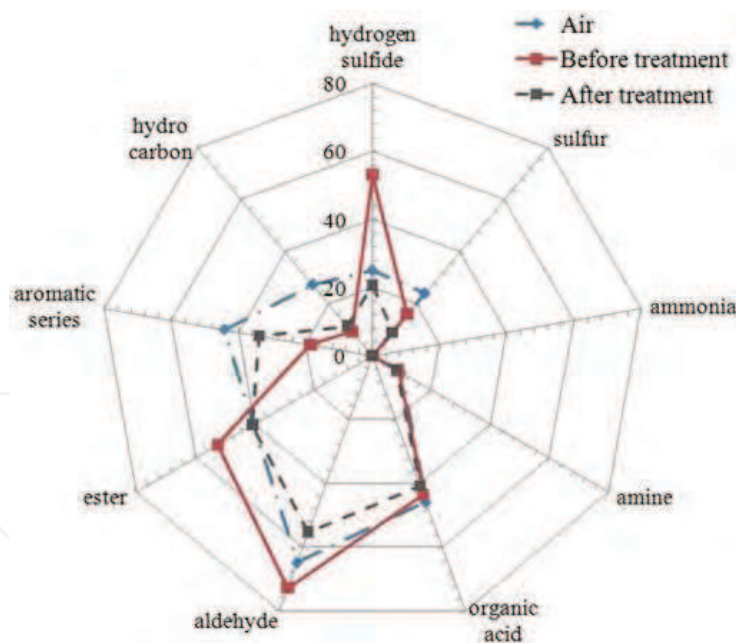

Fig. 22. Smell similarity before/after HCHO treatment and room air.

Sample gas was collected and analyzed by a Fragrance Flavor Analyzer, which has ten different semiconductor sensors with different sensitivities. Nine standard gases, which each have a different kind of smell, are input in this device and the analyzed sample gas is compared with them, providing data on the similarity against each standard gas. It is able to compare the change of the smell. The numbers in the radar graph stand for the similarity percentages against the nine standard gases(K. Shimizu et al., 2008).

Fig. 22 shows the smell similarity of simulated indoor air contained HCHO before and after the microplasma treatment for one pass process. Initial concentration of HCHO was set at 1ppm.

The smell of HCHO had a strong similarity with hydrogen sulfide, ester, and aldehyde. After microplasma treatment, the similarities of these three contents decreased, and the similarities with hydrocarbons and aromatics increased. It was observed that the smell of the sample gas changed to that of air after microplasma treatment.
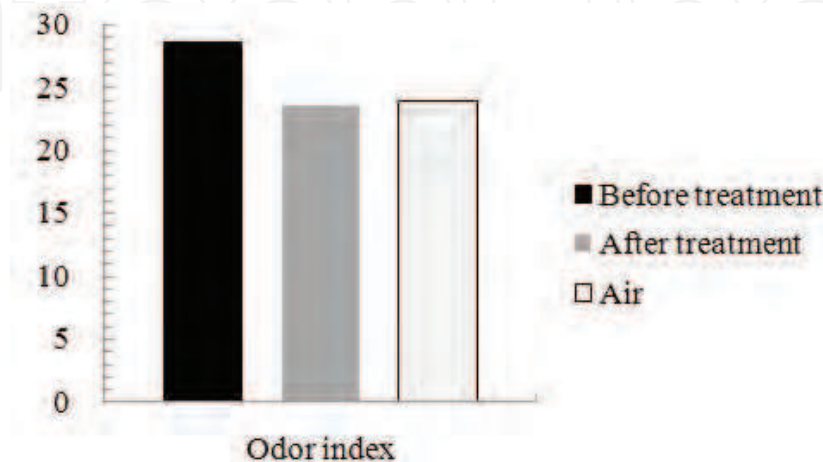

Fig. 23. The odor index before/after HCHO treatment and room air.

Fig. 23. shows the odor index before and after the microplasma one pass treatment, compared to that of room air. Odor index was about 29 before the microplasma treatment (Vd=1.24 kV), and after the microplasma treatment, it decreased to about 24. This value was slightly lower than the room air.

4.4 Sterilization of bacteria by microplasma

Virus or bacteria contained in tiny water droplets suspended in room air could cause serious illnesses such as influenza. One pass treatment of microplasma (shown in Fig. 7) can be an effective sterilization method for indoor air.

The diameters of the water particles formed by a medical nebulizer were measured by a laser particle counter (Kanomax, 3886). The gas flow rate was restricted to the range of 5–7 L/min because the pressure loss of the nebulizer was high. As shown in Fig. 24, a particle counter observed particles with diameters of 0.3 and 0.5 μm without water in the nebulizer. These particles could be the dust in the room air. With water added to the nebulizer, water droplets with diameters ranging from 0.5 to 5 μm were generated at the applied gas flow rates of 5, 6, and 7 L/min. Smaller water droplets did not coalesce to form larger droplets because the number of 0.5 μm droplets exceeds the number of 1.0 μm droplets. Since the sizes of colon bacilli *Escherichia coli* JCM20135 and *Bacillus subtilis* JCB 20036 are about 0.5 to 2.5 μm, they were contained within the water droplets generated by the nebulizer.

Inactivation of *Escherichia coli* and *Bacillus subtilis* were experimentally investigated at a total gas flow rate of 8.5 L/min by using microplasma electrodes. Ambient air and nitrogen were used to compare the effect of the oxidization effect of ozone and to confirm the effect of high electric field and UV radiation from microplasma.
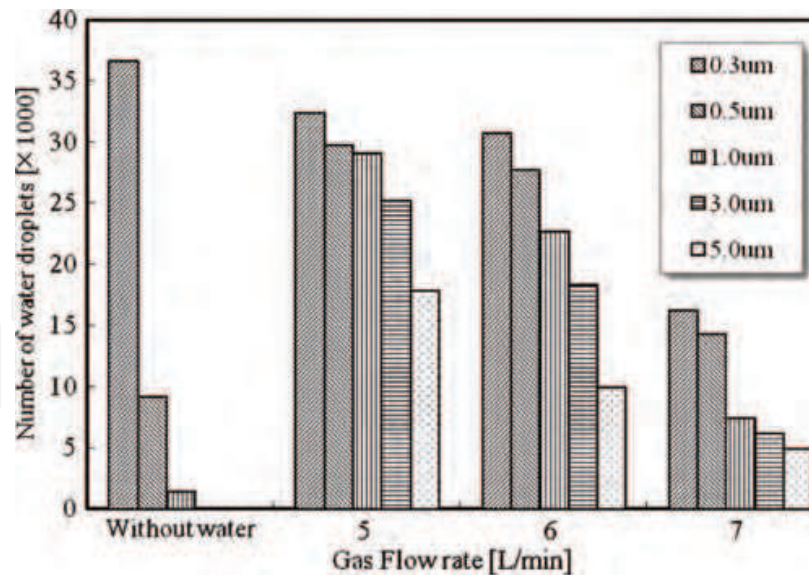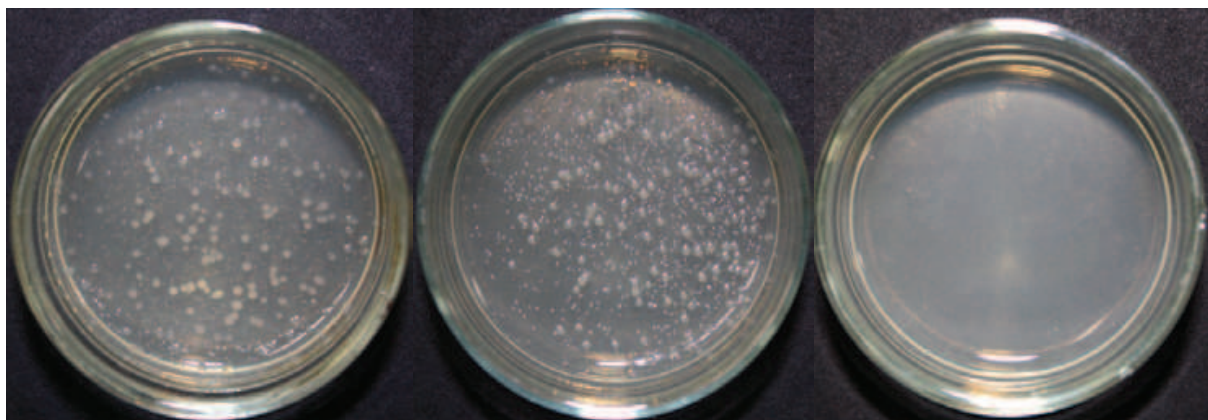
Fig. 24. Size distribution of water particles generated in by the nebulizer at gas flow rates of 5, 6, and 7 L/min.

Photographs of petri dishes with *E. coli*, before and after the microplasma treatment with air and nitrogen as the carrier gases, are shown in Fig. 25 and 26, respectively. *E. coli* was incubated at 37 degrees for 15 h after the microplasma treatment. Decrease of the colonies were observed both for air plasma and nitrogen plasma.
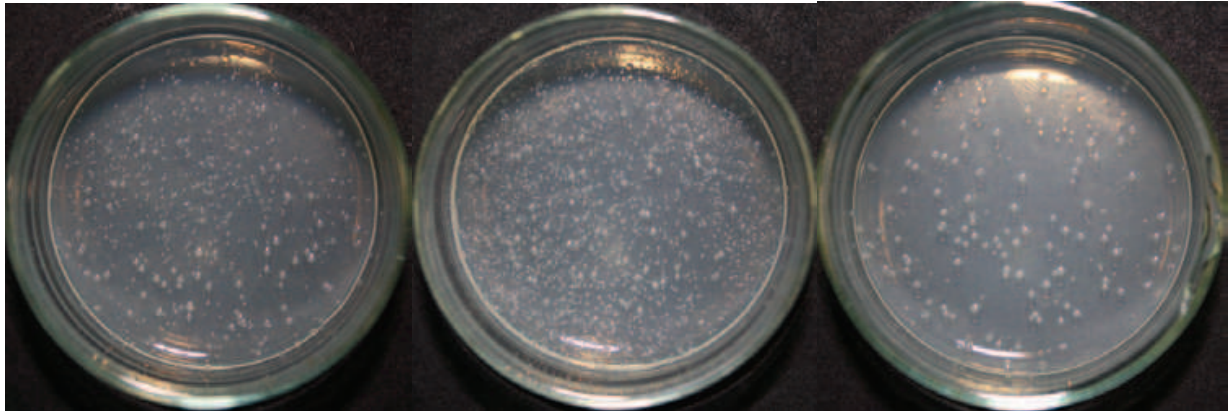

    (a) Before treatment.   (b) Discharge voltage 1.0 kV. (c) Discharge voltage 1.4 kV.

Fig. 25. Images of the *E.coli* samples before and after the air plasma treatment.

From these photos, air-plasma had better results to sterilize *E.coli* than that with nitrogen plasma. In the case of nitrogen as carrier gas, the presence of oxidation species such as ozone was not confirmed. This could explain the difference between air and nitrogen.

Photographs of petri dishes with *B.subtilis,* before and after the microplasma treatment with air and nitrogen as the carrier gases, are shown in Fig. 27 and 28, respectively. *B.subtilis* was incubated at 30 degrees for 18 h after the microplasma treatment. A decrease of the number of colonies was observed when the discharge voltage increased in both air plasma and nitrogen plasma. Decrease of the colonies was rather low compared to the of *E.coli* results. The inactivation process for bacteria may occur between the electrodes that generate microplasma or in the space near the electrodes after passing through the holes of the electrodes.
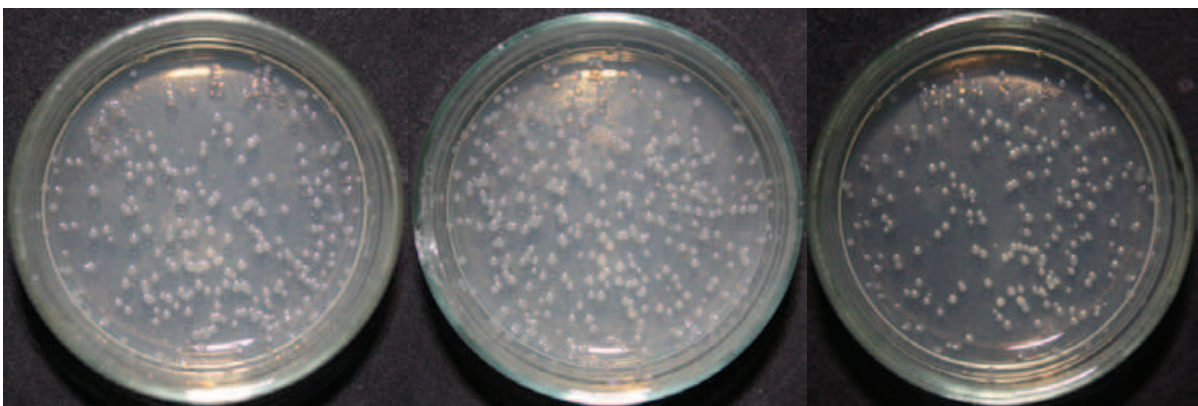
(a) Before treatment.   (b) Discharge voltage 1.0 kV.   (c) Discharge voltage 1.4 kV

Fig. 26. Images of the *E.coli* samples before and after the nitrogen plasma treatment.

(a) Before treatment.   (b) Discharge voltage 1.0 kV.   (c) Discharge voltage 1.4 kV.

Fig. 27. Images of the *B. subtilis* samples before and after the air plasma treatment.

(a) Before treatment.   (b) Discharge voltage 1.0 kV.   (c) Discharge voltage 1.4 kV.

Fig. 28. Images of the *B. subtilis* samples before and after the nitrogen plasma treatment.

As evident in these photos, more effective results were obtained for *E. coli* (gram-negative bacteria) than that of *B. subtilis*. Lower sterilization of *B. subtilis* (gram-positive bacteria) could be caused by its relatively impermeable cell walls, which have a thickness in the range

of 22 to 25 nm. The cell wall of gram-positive bacteria is composed of peptidoglycan and secondary polymers. Gram-negative bacteria have thin peptidoglycan layers (2–3 nm) plus an overlying lipid-protein bilayer (7–8 nm) known as the outer membrane (R. Stainer et al., 1986, T. Beveridge, 2001).
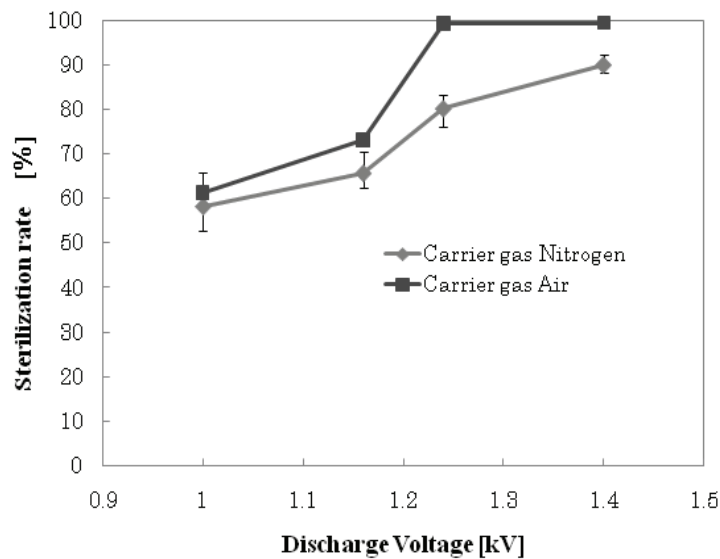

Fig. 29. Comparison of sterilization rate of *E.coli* with air and nitrogen plasma.

Sterilization rate of *E. coli* versus discharge voltages by air plasma and nitrogen plasma is shown in Figure 29. 100% sterilization of *E. coli* was accomplished with air as carrier gas for one pass treatment by microplasma as shown in Fig. 29. When nitrogen was the carrier gas, the sterilization rate surpassed 90% corresponding to a discharge voltage of 1.4 kV. Ozone was not formed during the discharge in the presence of nitrogen, and the sterilization of *E. coli* could be considered to be due to the effects of high electric field, excited nitrogen ions, active species such as OH, and UV radiation by microplasma, as described below in section 4.5.
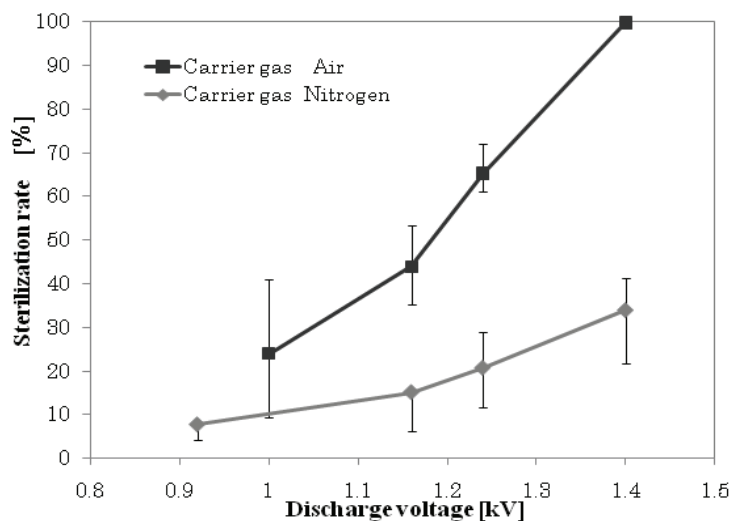

Fig. 30. Comparison of sterilization rate of *B. subtilis* with air and nitrogen plasma.

Sterilization rate of *B. subtilis* versus discharge voltage by air plasma and nitrogen plasma is shown in Fig. 30.

When air was used as carrier gas, maximum concentration of ozone was 22 ppm in the reactor. The effective reactor volume was 0.2 L, and the gas residence time of the reactor was about 1.4 seconds. When air was used as carrier gas, a near 100% sterilization rate of *B. subtilis* was achieved at discharge voltage of 1.4 kV. With nitrogen as the carrier gas, a sterilizaion rate of about 30% was achieved for *B. subtilis*. From this result, the sterilization process could be considered a synergetic effect of UV radiation, high electric field, (not only oxidative) radicals, and ozone. Various invesitigators show the sterilization effect (not by microplasma but) by atmospheric plasma or plasma jet (G. Fridman et al., 2008, M. G. Kong et al., 2009).
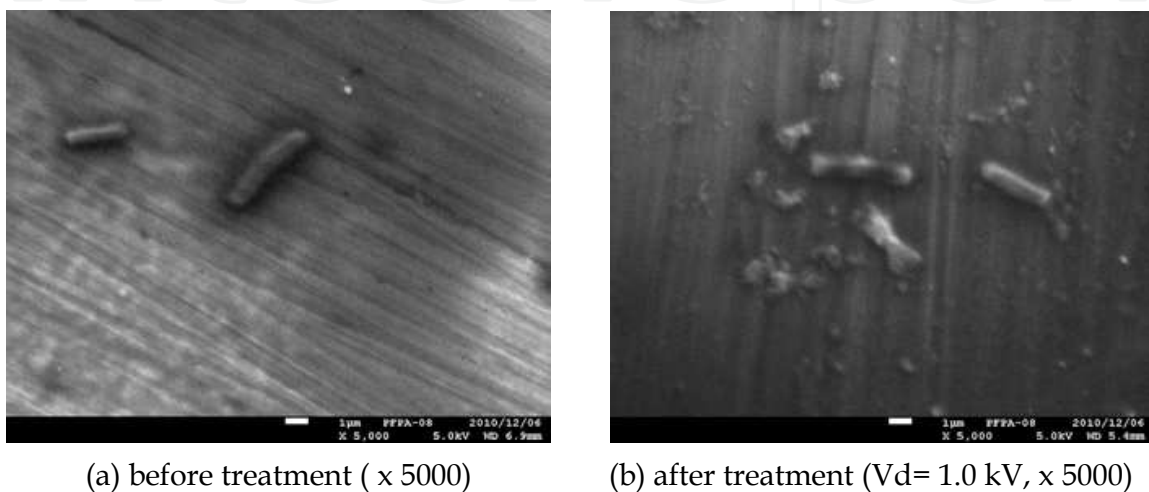

(a) before treatment (x 5000)   (b) after treatment (Vd= 1.0 kV, x 5000)

Fig. 31. Image of *B.subtilis* before and after the microplasma treatmnet.

Fig. 31 shows the images of *B. subtilis* before and after sterilization by microplasma. The images were taken by a Field Emission Scanning Electron Microscope (JOEL, JSM-7001F). Image (b) shows how the bacteria was affected by the microplasma discharge. The shape of the *B. subtilis* was changed and torn to pieces after the microplasma treatment. During the microplasma treatment process, every bacteria was exposed to a high electric field and UV

(a) Vd=800 V with air as carrier gas   (b) Vd=1000 V with air as carrier gas
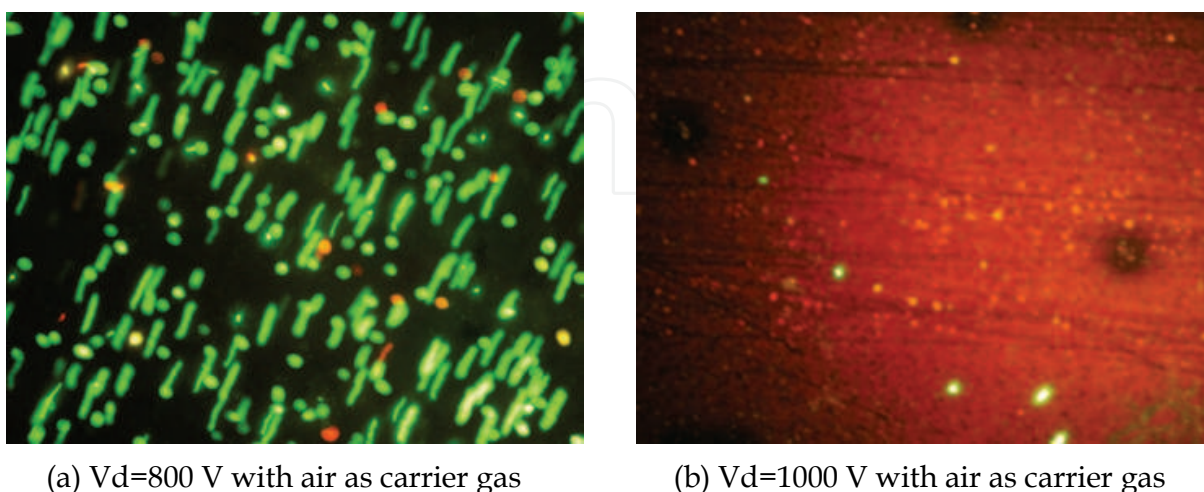
Fig. 32. *B. subtilis* spores (a) weak microplasma and (b) after microplasma treatment. Green and red florescences indicate intact and bleached membranes.

radiation while passing through the electrodes' holes generating microplasma. This could cause physical damage to the bacteria and affect their shape. In particular, active radical species had an etching effect to break cell walls, and UV affects the DNA directly to sever their structure (R. Stainer et al., 1986). Fig. 32 shows the bacteria (*B. subtilis*) damage by microplasma, where LIVE/DEAD BacLight Bacterial Viability Kits was used to identify intact and bleached membranes of *B. subtilis* spores with green and red florescence, respectively.

4.5 UV light emission by microplasma

UV light emissions from microplasma were observed to confirm the effect of UV light on the bacteria sterilization process (K. Shimizu et al., 2010). The emission spectra were measured by an intensified charge-coupled device (ICCD) camera (Ryoushi-giken, SMCP–ICCD 1024 HAM-NDS/UEmV), a spectrometer (Ryoushi-giken, VIS 351), and by a photomultiplier tube (Hamamatsu Photonics, R3896). A pulse generator (Tektronix, AFG 3021B) was used to trigger the ICCD camera and the Marx Generator consisting of semiconductor switches. A Marx Generator with four-stage MOSFET switches was used as the power supply. The spectrum was observed at -1.4 kV with a pulsewidth of 500 ns and a frequency of 1 kHz. The gas flow rate of dry nitrogen was set at 5 L/min. Data obtained from the ICCD camera were transferred to a computer for analysis.

Fig. 33 shows the emission spectrum of the microplasma discharge in N_2. Larger peaks indicate the N_2 second positive band system (N_2 SPS) and smaller peaks indicate the N_2 first negative band system (N_2 FNS). The spectrum indicates the generation of active molecular nitrogen species in the microplasma discharge (Z. Machala et al., 2007).
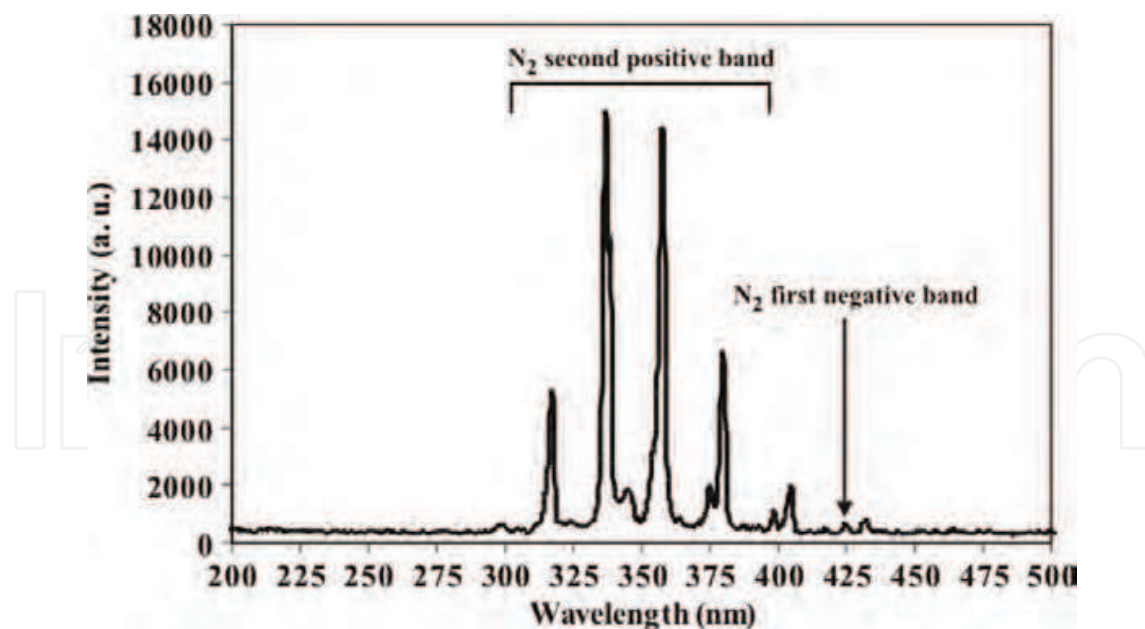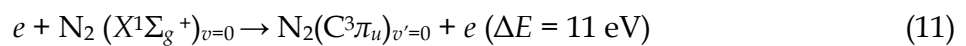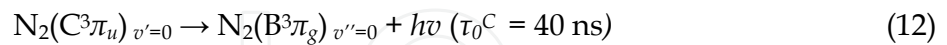

Fig. 33. Spectrum of N_2 second positive band system and N_2 first negative band system by microplasma discharge in nitrogen. Gas flow rate was set at 5 L/min.

The elementary processes (11) and (12) describe the radiation kinetics for the N_2 SPS with a wavelength of 337.1 nm and at atmospheric pressure (K. V. Kozlov and H.-E. Wagner, 2007).

The excitation of nitrogen molecules in the ground state by direct electron impact is described by

$$e + N_2 \, (X^1\Sigma_g{}^+)_{v=0} \rightarrow N_2(C^3\pi_u)_{v'=0} + e \; (\Delta E = 11 \text{ eV}) \tag{11}$$

The spontaneous radiation of nitrogen in the excited state is described by

$$N_2(C^3\pi_u) \,_{v'=0} \rightarrow N_2(B^3\pi_g) \,_{v''=0} + hv \; (\tau_0{}^C = 40 \text{ ns}) \tag{12}$$

Water droplets from the nebulizer were entrained in the nitrogen gas that entered the chamber to confirm another active species in the microplasma discharge. Fig. 34 shows the emission spectrum of nitrogen with entrained water droplets.
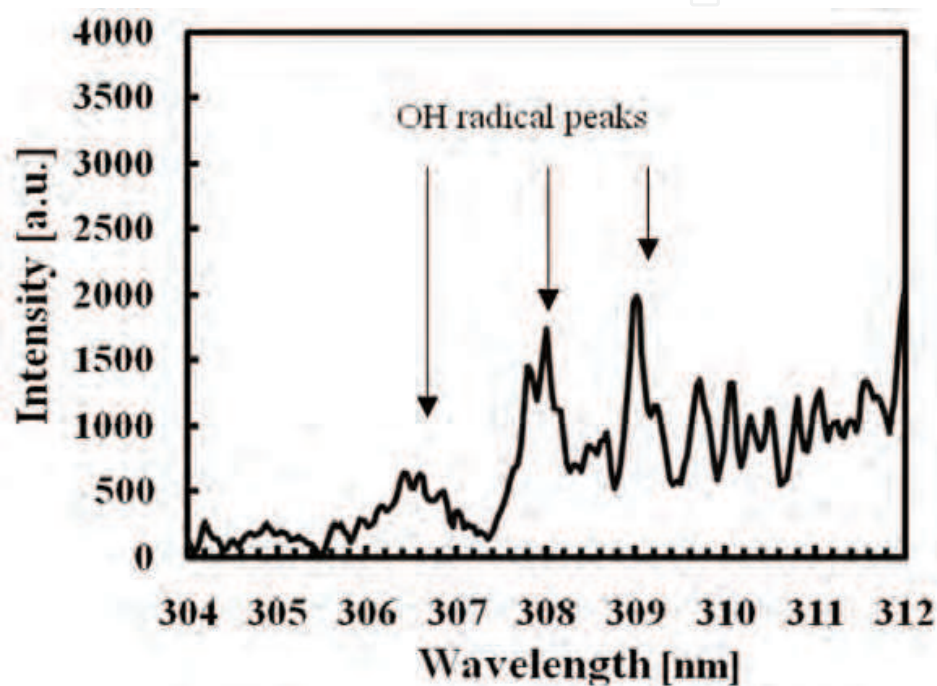

Fig. 34. OH radical peaks of emission spectrum of microplasma discharge in nitrogen with H_2O by an HV amplifier at 1.44 kV. Gas flow rate was set at 5 L/min.

The UV light emission confirmed active species such as OH radicals measured at 306.4 nm, 307.8 nm and 308.9 nm (Z. Machala et al., 2007, F. Liu et al., 2007). UV light emissions from 316 nm and higher wavelengths were also observed, which affect the sterilization process of bacteria (J. M. C. Robertson et al., 2005, A. K. Benabbou et al., 2007). OH radicals are generated via electron impact dissociation of H_2O which leads to the production of H and OH radicals:

$$e + H_2O \rightarrow e + H + OH \tag{13}$$

Also, the excited state $O(^1D)$ dissociated H_2O to generate OH:

$$O(^1D) + H_2O \rightarrow 2 \, OH \tag{14}$$

Thus OH radical peak was obtained in the presence of H_2O in air or in nitrogen. The combination of UV light and active species could have contributed to the sterilization process of bacteria in air.

5. Conclusions and future work

Indoor air control a keen issue worldwide, since pandemics such as new influenza strains are now serious problems in every country. People are also worrying about smells or odours in homes, offices, hospitals, hotels, on trains etc. Various devices which claim to generate ozone or ions to control indoor air are on the market now. But their performances are insufficient, especially for air pollutant removal (A. Nozaki et al., 2010). Mechanisms for the removal of air pollutants or bacteria are still not proven, especially for reactions with coagulated aerosols in the air in so called "clustered ions" emitted by indoor air control devices (T. Yamauchi et al., 2007). Such mechanisms require more research to improve the performances of indoor air control devices.

In this chapter, a technique for indoor air control by microplasma was presented with the various data for VOCs removal with low concentration of ozone and bacteria sterilization in one pass treatment. Smell analysis and byproduct analysis were also presented to evaluate the microplasma process. Also, various power supplies including a self-made Marx Generator are presented resulting in low ozone concentration in output gas. It is also important to treat indoor air in such a way as to not generate gas harmful to human beings. Moreover, microplasma has various features as discussed in "2. About Microplasma". Discharge voltage is lower than that of other nonthermal plasma methods, or other indoor air control devices on the market. This means microplasma devices will possibly be made small, light and cost effective for commercial production. Air control devices generate ions to treat room air; in contrast, microplasma can treat room air, while room air flows into the microplasma electrode. There could be UV light emission, active species, strong electrical field between the electrodes. Odor gas molecules, bacteria or viruses could be decomposed or sterilized here.

Mechanisms of VOCs removal or sterilization process have also been demonstrated with chemical reactions and emission spectra which could attribute emitting active species such as OH radicals from microplasma. But this data is still insufficient to explain these mechanisms.

In this chapter, there is no information about ion density generated by microplasma. Ions could be generated during the microplasma process. However evidence supporting claims that ions contribute to indoor air treatment processes is still not overwhelmingly conclusive. Further study is required to show these reaction processes or sterilization processes by microplasma are "effective", and how safe this process is for practical use in home appliances.

6. References

A. Mizuno, K. Shimizu, A. Chakrabarti, L. Dascalescu, and S. Furuta. (1995). NOx Removal Process Using Pulsed Discharge Plasma, *IEEE Trans. on IAS*, Vol. 31, No. 5, pp. 957-963

A. Nozaki, Y. Ichijo, and Y. Narita. (2010). A Study on the Indoor Air Pollutant Removal Performance of Room Air Cleaners, *Proc. Int'l. Symp. On Contamination Control 2010,* Tokyo, pp. 505-510

A. K. Benabbou, Z. Derriche, C. Felix, P. Lejeune, and C. Guillard. (2007). Photocatalytic inactivation of Escherischia coli: Effect of concentration of TiO2 and microorganism, nature, and intensity of UV irradiation, *Appl. Catalysis B, Environ.*, vol. 76, no. 3/4, pp. 257–263, Nov, 2007

A. Koutsospyros, S.-M. Yin, C. Christodoulatos and K. Becker. (2004). Destruction of Hydrocarbons in Non-thermal, Ambient-Pressure, Capillary Discharge Plasmas, Int. J. Mass. Spectrum., vol. 233, pp. 305-315

A. Sakudo, H. Shintani. (2010). *Sterlization and Disinfection by Plasma*, Nova Science Publishers, Inc., New York.

A. Seki, T. Takigawa, R. Kishi, K. Sakabe, S. Torii, M. Tanaka, T. Yoshimura, K. Morimoto, T. Katoh, S. Kira and Y. Aizawa. (2007). Review of 'Sick House Syndrome', *Jpn. J. Hyg*, Vol. 62, pp. 939-948

A. Rousseau , L. V. Gatilova, J. Röpcke, A. V. Meshchanov and Y. Z. Ionikh. (2005). NO and NO_2 production in pulsed low pressure dc discharge, *Appl. Phys. Let.*, vol.86, pp. 2115011-2115013

B. Eliasson, M. Hirth and U. Kogelschatz. (1987). Ozone synthesis from oxygen in dielectric barrier discharge, *J. Phys. D: Appl. Phys.*, vol. 20, pp. 1421-1437

D. li, D. Yakushiji, S. Kanazawa, T. Ohkubo and Y. Nomoto.(2002). Decomposition of Toluene by Streamer Corona Discharge with Catalyst, *J. Electrost.*, vol. 55, pp. 311-319

Daikin company website: http://www.daikin.com/global_ac/products/residential/airpurifier_mc707/mechanism.html

D. G. Storch and M. J. Krushner. (1993). Destruction mechanisms for formaldehyde in atmospheric pressure low temerpature plasmas, *J. Appl. Phys,* vol. 73, no. 1

F. J. Trompeter, W. J. Neff, O. Franken, M. Heise, M. Neiger, S. Liu, G. J. Pietsch, and A. B. Saveljew. (2002). Reduction of Bacillus Subtilis and Aspergillus Niger Spores Using Nonthermal Atmospheric Gas Discharges, *IEEE Trans. on plasma science,* Vol.30, No. 4, pp. 1416-1423

F. Liu, W. Wang, S. Wang, W. Zheng, and Y. Wang. (2007). Diagnosis of OH radical by optical emission spectroscopy in a wire-plate bi-directional pulsed corona discharge, *J. Electrostat.*, vol. 65, no. 7, pp. 445–451, Jun, 2007

G. Fridman, G. Friedman, Al. Gutsol, A. B. Shekhter, V. N. Vasilets, A. Fridman. (2008). Applied Plasma Medicine, *Plasma Process. Polym.*, Vol. 5, 503–533

H. Ghomi, M. S. Rahman, P. R. Chalise, Y. Hayashi, M. Watanabe, A. Okino, T. Ano, M. Shoda and E. Hotta. (2005). Experimental Investigation of Effect of Low-Energy Pulsed Atmospheric Electron Beam on Bacterial Cells, *Jpn. J. Appl. Phys,* Vol. 44, No. 12, pp. 8698-8701

H. X. Ding, A. M. Z., X. F. Yang, C. H. Li, and Y. Xu. (2005). Removal of formaldehyde form gas streames via packed-bed dielectric barrier discharge plasmas, *J. Phys. D: Appl. Phys*, vol. 38, pp. 4160-4167

H. Yoshida, Z. Marui, M. Aoyama, J. Sugiura and A. Mizuno. (1989). Removal of Ordor Gas Component Utilizing Plasma Chemical Reactions Promoted by the Partial Discharge in a Ferroelectric Pellet Layer, *J. IEJ*, vol. 13, no. 5

J. Kitayama and M. Kuzumoto. (1997). Theoretical and experimental study on ozone generation charcteristics of an oxygen-fed ozone generator in silent discharge, *J. Phys. D:Appl. Phys.*, vol. 30, pp. 2453-2461

J. M. C. Robertson, P. K. J. Robertson, and L. A. Lawton. (2005). A comparison of the effectiveness of TiO_2 photocatalysis and UVA photolysis for the destruction of three pathogenic micro-organisms, *J. Photochem. Photobiol. A, Chem.*, vol. 175, no. 1, pp. 51–56

K. Kitano, H. Aoki, S. Hamaguchi. (2006). Radio-Frequency-Driven Atmospheric-Pressure Plasmas in Contact with Liquid Water, *Jpn. J. Appl. Phys,* Vol. 45, No. 10, pp. 8294-8297

K. N. Faungnawakji, D. Sano, T. Yamamoto, T. Kanki, T. Charinpanitkul and W. Tanthapanichakoon. (2004). Removal of Acetaldehyde in Air Using a Wetted-Wall Corona Discharge reactor, *Chem.Eng.J.,* vol.103, pp.115-122

K. Shimizu, M. Yamada, M. Kanamori, and M. Blajan. (2010a) Basic Study of Bacteria Inactivation at Low Discharge Voltage by Using Microplasmas, *IEEE Trans. on IAS,* Vol. 46, No. 2, pp. 641-649

K. Shimizu, M. Kanamori, and M. Blajan. (2010b). Application of Atmospheric Microplasma for Indoor Air Treatment, *IJPEST,* Vol. 4, No. 1, pp. 45-51

K. Shimizu, T. Ishii, and M. Blajan. (2010c). Emission Spectroscopy of Pulse Power Microplasma for Atmospheric Pollution Control, *IEEE Trans. on IAS,* Vol. 46, No. 3, pp. 1125-1131

K. Shimizu, T. Sugiyama, M. Nishamani L. S. and M. Kanamori. (2009). Application of Micro Plasma for NOx Removal, *IEEE Trans. on IAS,* Vol. 45, No. 4, pp. 1506-1512

K. Shimizu, T. Sugiyama, and L. S. Manisha Nishamani. (2008). Study of Air Pollution Control by Using Micro Plasma Filter, *IEEE Trans. on IAS,* Vol. 44, No. 2, pp. 506-511

K. Shimizu, T. Sugiyama and M. Kanamori. (2008). Application of microplasma for ozone generation and environmental protection, *IJPEST,* vol. 2, no. 1, pp.38-43

K. Tachibana. (2006). Current Status of Microplasma Research, *IEEJ Trans.,* Vol. 1, pp. 145-155

K. Urashima and J. S. Chang. (2000). Removal of Volatile Organic Compounds from Air Streams and Industrial Flue Gases by Non-thermal Plasma Technology, *IEEE Dielec. Elect. Insul.,* vol. 7, pp. 602-613

K. V. Kozlov and H.-E. Wagner. (2007). Progress in spectroscopic diagnostics of barrier discharges, *Contrib. Plasma Phys.,* vol. 47, no. 1/2, pp. 26–33, Feb, 2007

L. A. Rosocha, G. K. Anderson, L. A. Bechtold, J. J.Coogan, H. G. Heck, M. Kang, W. H. McCulla, R. A. Tennant, and P. J. Wantuck. (1993). Treatment of Hazardous Organic Wastes Using Silent Discharge Plasmas, *Non-thermal Plasma Techniques for Pollution Control*, NATO ASI Ser. 34, Part B, Springer-Verlag Pub., Oxford, pp. 281-308

M. Blajan, S. Muramatsu, T. Ishii, H. Mimura, and K. Shimizu. (2010). Emission Spectroscopy of Microplasma Driven by a Pulsed Power Supply, *Journal of the Institute of Electrostatics Japan,* Vol. 34, No. 2, pp. 99-104, 2010, ISSN 0386-2550

M. Blajan, A. Umeda, S. Muramatsu, K. Shimizu. (2010). Emission spectroscopy of pulsed powered microplasma for surface treatment of PEN film, *Proc. of 2010 IEEE Industry Applications Society Annual Meeting,* CD-ROM, 3-7 October 2010 Houston, Texas, USA, Digital Object Identifier: 10.1109/IAS.2010.5614482

M. Blajan, T. Ishii, H. Mimura, K. Shimizu. (2009). Emission spectrometry of microplasma for NOx removal process, *Book of abstracts ISPC 19 International Symposium on Plasma Chemistry,* Ruhr-University Bochum, Germany, July 27 - 31 (2009) 398

M. Laroussi, G. S. Sayler, B. B. Glascock, B. McCurdy, M. E. Pearce, N. G. Bright, and C. M. Malott. (2004). Images of Biological Samples Undergoing Sterilization by a Glow Discharge at Atmospheric Pressure, *IEEE Transactions on plasma science,* Vol.27, No. 1, pp. 34-35

M. G. Kong, G Kroesen, G Morfill, T Nosenko, T Shimizu,J van Dijk and J L Zimmermann. (2009). Plasma medicine: an introductory review, *New Journal of Physics,* Vol. 11, pp. 1-35

M. Nagatsu, F. Terashita and Y. Koide. (2003). "Low-Temperature Sterilization with Surface-Wave-Excited Oxygen Plasma", Jpn. J. Appl. Phys, Vol. 42, No. 7B, pp. 856-859

N. Hayashi, W. Guan, S. Tsutsui, T. Tomari and Y. Hanada. (2006). Sterilization of Medical Equipment Using Radicals Produced by Oxygen/Water vapor RF Plasma, *Jpn. J. Appl. Phys,* Vol. 45, No. 10B, pp. 8358-8363

N. S. Panikov, S. Paduraru, R. Crowe, P. J. Ricatto, C. Christodoulatos, and K. Becker. (2002) Destruction of Bacillus Subtilis Cells Using an Atmospheric-Pressure Capillary Plasma Electrode Discharge, *IEEE Trans. on plasma science,* Vol. 30, No. 4, pp. 1424-1428

P. Wolkoff, G. D.Nielsen. (2001). Organic compounds in indoor air- their relevance for perceived indoor air quality?, *Atmospheric Environment*, Vol. 35, pp. 4407 – 4417

Panasonic company website: http://www.peshk.panasonic.hk/ap/index.html

R. Atkinson, D. L. Baulch, R. A.Cox, J. N. Crowley, R. F. Hampson, R. G. Hynes, M. E. Jenkin, M. J. Rossi, and J. Troe. (2004). Evaluated kinetic and photochemical data for atmospheric chemistry: Volume 1 – gas phase reactions of Ox, HOx NOx and SOx species, *Atomos. Chem. Phys.*, Vol.4, pp. 1461 – 1738

R. Atkinson, D. L. Baulch, R. A.Cox, J. N. Crowley, R. F. Hampson, R. G. Hynes, M. E. Jenkin, M. J. Rossi, and J. Troe. (2006). Evaluated kinetic and photochemical data for atmospheric chemistry: Volume 2 – gas phase reactions of organic species, *Atmos. Chem. Phys.*, Vol.6, pp. 3625 – 4055

R. Stainer, J. Ingraham,M.Wheelis, and P. Painter. (1986). *The Microbial World.*, 5th ed. New York: Prentice-Hall

S. Agnihotri, M. P. Cal, and J. Prien. (2004). Destruction of 1,1,1-Trichloroethane Using Dielectric Barrier Discharge Nonthermal Plasma, *J. Env. Engg.*, pp. 349-354

Sharp company website: http://www.sharp.ca/products/ion/plasma_home.asp

T. Beveridge. (2001). "Use of the Gram stain in microbiology," *Biotech Histochem.*, vol. 76, no. 3, pp. 111–118, May, 2001

T. Ito, Y. Murayama, M. Suzuki, N. Yoshimura, K. Iwano and K. Kudo. (1992). Evidence for sterilization of Saccharomyces Cerevisiae K 7 by an External Magnetic Flux, *Jpn. J. Appl. Phys,* Vol. 31, No. 6A, pp. 676-678

T. Kuroki, M. Okubo and T. Yamamoto. (2001). Indoor Air Cleaning Technology Using Non-equilibrium Plasma, *JSME. Trans. B,* vol. 67, no. 658, Jun, Japan

T. Oda, K. Yamaji, and T. Takahashi. (2004). Decomposition of Dilute Trichloroethylene by Nonthermal Plasma Processing ~Gas Flow Rate, Catalyst, and Ozone Effect, *IEEE Trans. Ind. Appl.*, vol. 40, pp. 430-436

T.C. Montie, K. Kelly-Wintenberg, J. R. Roth. (2000). An overview of research using the one atmosphere uniform glow discharge plasma (OAUGDP) for sterilization of surfaces and materials, *IEEE Trans. Plasma Sci,* Vol. 28, pp. 41-50

T. Yamauchi, H. Suda, and Y. Matsui. (2007). Development of Home Appliances Using Electrostatic Atomization, *J. Aerosol Res.*, vol. 22, pp. 5-10

U. Kogelschatz. (2007). Applications of Microplasmas and Microreactor Technology, *Contrib. Plasma Phys.* Vol. 47, No. 1-2, pp. 80-88

Y.-H. Song, S.-J. Kim, K.-I. Choi and T. Yamamoto. (2002). Effect of adsorption and temperature on a nonthermal plasma plasma process for removing VOCs, *J. Electrost.*, vol. 55, pp. 189-201

Z. Machala, M. Janda, K. Hensel, I. Jedlovský, L. Leštinská, V. Foltin, V. Martišovitš, and M. Morvová. (2007). Emission spectroscopy of atmospheric pressure plasmas for bio-medical and environmental applications, *J. Mol. Spectrosc.*, vol. 243, no. 2, pp. 194–201

Advanced Air Pollution

Edited by Dr. Farhad Nejadkoorki

Leading air quality professionals describe different aspects of air pollution. The book presents information on four broad areas of interest in the air pollution field; the air pollution monitoring; air quality modeling; the GIS techniques to manage air quality; the new approaches to manage air quality. This book fulfills the need on the latest concepts of air pollution science and provides comprehensive information on all relevant components relating to air pollution issues in urban areas and industries. The book is suitable for a variety of scientists who wish to follow application of the theory in practice in air pollution. Known for its broad case studies, the book emphasizes an insightful of the connection between sources and control of air pollution, rather than being a simple manual on the subject.

How to reference

In order to correctly reference this scholarly work, feel free to copy and paste the following:

INTECH
open science | open minds